Exciton-polariton integrated circuits

T. C. H. Liew,[1] A. V. Kavokin,[2] T. Ostatnický,[2] M. Kaliteevski,[3] I. A. Shelykh,[4,5] and R. A. Abram[3]

[1]*Institute of Theoretical Physics, Ecole Polytechnique Fédérale de Lausanne (EPFL), CH-1015 Lausanne, Switzerland*
[2]*Physics and Astronomy School, University of Southampton, Highfield, Southampton SO17 1BJ, United Kingdom*
[3]*Department of Physics, Durham University, Durham DH1 3LE, United Kingdom*
[4]*Science Institute, University of Iceland, Dunhagi 3, IS-107 Reykjavik, Iceland*
[5]*International Institute of Physics, Av. Odilon Gomes de Lima 1722, 59078-400, Natal, Brazil*

We show that logical signals encoded in bistable states in semiconductor microcavities can be generated and controlled electronically by exploiting the electrical sensitivity of Tamm-plasmon–exciton-polariton modes. The signals can be transported along polariton neurons, created with a patterned metal surface. Using the Gross-Pitaevskii equations, we simulate an electrically controlled transistor and find that high repetition rates (10 GHz) are possible.

PACS number(s): 71.36.+c, 42.55.Sa, 42.65.Pc

Exciton-polaritons are part-light part-matter quasiparticles which govern the optical properties of semiconductor crystals at low temperature.[1] Recently, a number of fascinating effects related to exciton-polaritons have been discovered in semiconductor microcavity structures where a confined optical mode is brought into resonance with an excitonic transition. The fundamental discoveries of the Bose-Einstein condensation[2–4] of exciton-polaritons and their superfluidity[5] at elevated temperatures have paved the way toward the realization of a new generation of optoelectronic devices.[6] From the technological point of view the nonlinear optical effects linked with exciton-polaritons are of particular interest. The recently demonstrated optical bistability in a biased microcavity with an extraordinarily low switching power[7] demonstrates the feasibility of optical integrated circuits based on "polariton neurons" in planar microcavities.[8] In order to produce such devices, exciton-polaritons in microcavities must be confined in lateral channels, where the propagation of domains of high-density exciton-polariton liquid may be controlled by external light or electrical bias. Recently it was shown that such channeling of polaritons is possible using hybrid Tamm-plasmon–exciton-polariton modes (TPEPMs) which are formed under thin metallic stripes deposited on the top of a planar semiconductor microcavity.[9–11] TPEPM states are redshifted from the bare cavity polariton modes by several meV, which provides efficient one-dimensional confinement. Exciton-polariton transistors, switches, and logic gates based on TPEPMs would operate at gigahertz frequencies, have extremely low switching power, and be easily integrated on a chip.

The development of practical optical integrated circuits would represent a revolutionary breakthrough in modern optoelectronics, making possible ultrafast information processing with extremely low losses. However, the realization of optical integrated circuits is a complex task which cannot be achieved without exploiting new physical effects, device concepts, and technological approaches. We propose exploiting the newly discovered effects of polariton-mediated optical bistability, plasmon-polariton coupling, and propagation of polariton domain walls in microcavities in a concept of an optical integrated circuit. It is based on several ideas, namely: (i) bistable switching of the optically driven polariton state due to nonlinear polariton-polariton interactions,[12] which has been experimentally observed recently;[13,14] (ii) channeling of polaritons below metallic stripes due to the hybridization of the Tamm-plasmon states and cavity exciton-polaritons; (iii) electrical control of the detuning between the exciton-polariton mode and the pumping laser due to the quantum confined Stark effect; and (iv) propagation of domain walls between different bistable states.

Polariton transistor scheme. Figure 1(a) shows schematically our proposed building block of future polariton integrated circuits: a polariton spin transistor. The figure illustrates a conventional planar microcavity in which Bragg mirrors confine light so that it interacts strongly with excitons in a quantum well. However, in addition our structure has a patterned metal structure on the top surface, comprising a chain of four segments. The band structure of exciton-polariton modes in a microcavity can be strongly affected by the presence of a metallic layer on the top of the structure [as apparent in Fig. 1(c)], and this can be used to provide the lateral confinement necessary for integrated circuits. The thicknesses of the metallic layer and of the semiconductor layer next to it determine the energy of the Tamm-plasmon mode localized at the metal-Bragg mirror interface.[9–11] If the Tamm plasmon is strongly detuned from the cavity polariton modes, the effect of the metal is to blueshift the cavity modes by ~ 0.4 eV.[4] On the other hand, if the Tamm plasmon is put in resonance with the cavity polaritons, a new hybrid TPEPM can appear, which has components of the exciton state, cavity photon, and Tamm plasmon. The lowest TPEPM is redshifted with respect to the lowest bare cavity polariton mode, with the size of the shift dependent on the exciton oscillator strength and the parameters of the Bragg mirror between the cavity and metal.[11] For applications in polariton integrated circuits at low temperatures, a shift of about 5 meV would provide sufficient lateral confinement, and this can be easily achieved in GaAs-based structures. For room-temperature operation, the larger lateral confinement potential necessary can be achieved in GaN-based systems. Selective optical excitation of the TPEPM is achieved by tuning the photon energy of a continuous-wave (cw) laser to lie between the lowest TPEPM and the lowest cavity polariton mode outside the channel. In this case, there is no absorption of light in the regions of the sample not covered by metal. TPEPMs are confined in the channels and the lowest TPEPM
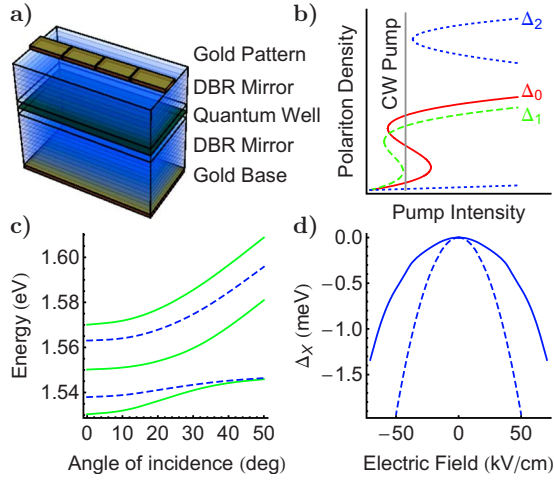
FIG. 1. (Color online) (a) Schematic diagram of a semiconductor microcavity with metallic electrodes used to realize an electrically controlled polariton neuron. A strip of metal on the surface is divided into four segments, which are individually connected to an electrical supply (not shown) allowing the polariton potential to be changed in each segment. Note that the diagram is not to scale; in reality the lateral size of the metal strip is larger than the height of the structure. (b) Dependence of the polariton density on the optical pump intensity for different values of the detuning ($\Delta_1 < \Delta_0 < \Delta_2$) between the optical pump photon energy and the lower polariton energy. The detuning can be changed in the different segments by varying the applied electric potential. For a pump intensity close to the vertical gray line, switching between the different curves can have a major effect on the polariton density. (c) Dispersion relation for cavity polaritons (blue dashed curve) and hybrid TPEPM (green solid curve). The lowest-energy hybrid state is redshifted by several meV with respect to the lowest polariton mode in the vicinity of metal overlay, providing localization of exciton-polaritons in the channels below the metallic segments. (d) Redshift of the ground TPEP modes (solid curve) and exciton modes (dashed curve).

absorbs laser light only if its energy is tuned to the laser energy. This tuning can be achieved and controlled by the application of an electric field across the cavity (in the direction normal to the cavity plane). An electric field affects the exciton energy and oscillator strength due to the quantum confined Stark effect, which leads to the shift of the TPEPMs as well. Electric fields to control the local TPEPM energy selectively can be produced by applying a potential difference relative to the structure's back contact to one or more of the four metallic segments.

Figure 1(b) shows the response of the polariton density to the intensity of a circularly polarized cw optical pump. The different curves represent the cases of different detunings between the optical pump photon energy and the lowest TPEPM energy (we define the detuning as that measured in the low-density regime rather than defining a renormalized detuning). By varying the electrical potential applied to a segment the detuning in its locality can be varied and a particular response as represented by the curves in Fig. 1(b) can be selected [an increase in the applied electric field causes an increased redshift of the TPEPM energy as shown in Fig. 1(d); see also discussion below]. We consider a device with the initial condition that all segments have the same applied

potential and hence the same detuning Δ_0. Illuminating the whole system by a broad area optical pump, each segment is initially in a low polariton density state of the TPEPM [given by the intersection between the vertical gray line and the lower branch of the (red) solid curve in Fig. 1(b)].

A signal in the structure can be triggered by lowering the potential applied to the first segment so that the local detuning is reduced to the value Δ_1, corresponding to the (green) dashed S-shaped curve in Fig. 1(b). We expect the change in the potential to cause a major increase in the polariton density [given by the point where the vertical gray line intersects the (green) dashed curve]. Furthermore, polaritons have a particularly light effective mass, which allows them to propagate over micron-scale distances during their short lifetime. The high population of polaritons in the first segment thus begins to spread, tunneling across the narrow gap into the second segment. As a result the increasing polariton population in the area just inside the second segment switches to the upper branch of the (red) solid S-shaped curve in Fig. 1(b). This switching effect continues across the whole segment and indeed across segments later in the chain. In analogy with biological neurons, the signal is carried as a propagating change in the state of the system along the channel. While the signal of a biological neuron is encoded as a switch in the relative concentrations of charged ions across the axon membrane, a polariton neuron encodes the signal as a switch in the local polariton density. Note that just as biological neurons do not rely on charged ions traveling down the whole length of the neuron, the same is the case with polaritons in polariton neurons. Therefore, the signal can propagate substantially further than the distance a single polariton can be expected to travel—in fact the signal is able to propagate to the edge of the cw optical field.

Exciton redshift due to an applied electric field. Before presenting theoretical modeling of our proposed device, we give details on how the exciton redshift can be related to an applied electric field. Although excitons localized in the quantum well are electrically neutral, their components (electrons and holes) have opposite electric charges and therefore interact with the electric field. As a result, an applied electric field leads to distortion of the exciton wave function and to the change in the exciton energy and the exciton oscillator strength.[15–17] To determine the exciton energy, we use the model of Ref. [16] with a separable exciton trial wave function of the form

$$\Psi(\vec{r}_e, \vec{r}_h, z_e, z_h) = \Psi_\parallel(\vec{r}_e, \vec{r}_h)\Psi_e(z_e)\Psi_h(z_h), \qquad (1)$$

where the unperturbed exciton in-plane wave function is

$$\Psi_\parallel(\vec{r}_e, \vec{r}_h) = \sqrt{\frac{2}{\pi a_B^2}}\exp\left\{-\frac{|\vec{r}_e - \vec{r}_h|}{a_B}\right\}, \qquad (2)$$

in which a_B is the two-dimensional exciton Bohr radius and $\vec{r}_{e,h}$ are the in-plane components of the electron and hole spatial coordinates. The wave functions Ψ_e and Ψ_h describe the electron and hole wave function behaviors in the direction normal to the quantum well plane (the spatial coordinates are denoted as z_e and z_h for electrons and holes, respectively). The appropriate Hamiltonian for the problem is
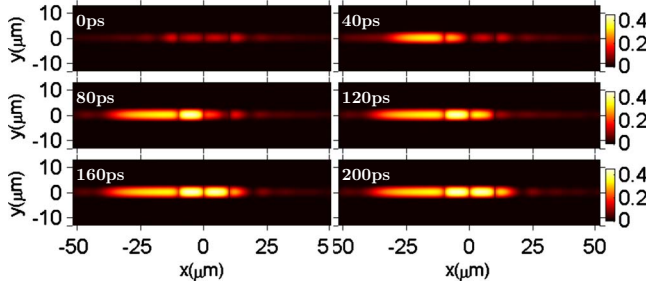
FIG. 2. (Color online) Response of the polariton intensity in the microcavity plane when the potential in the first segment is altered such that the pump-polariton detuning is changed from Δ_0 = 0.5 meV to Δ_1 = 0.4 meV. Initially the intensity in the first segment increases. Polaritons then propagate into the second region where there is a switching to the higher intensity state allowed by bistability. The polariton signal continues to a distance limited by the extent of the optical pump (which has a 40 μm half-width at half-maximum in the x direction in the calculation).

$$\mathcal{H} = \frac{p_e^2}{2m_e(z_e)} + \frac{p_h^2}{2m_h(z_h)} + V_e(z_e) + V_h(z_h)$$
$$- eFz_e + eFz_h - \frac{e^2}{\epsilon(|z_e - z_h|^2 + |\vec{r}_e - \vec{r}_h|^2)}, \quad (3)$$

where the particle momenta are denoted by operators $p_{e,h}$, their masses (depending on the particle position either in the well or in the barrier) are $m_{e,h}$, and the quantum well confining potentials are $V_{e,h}$. The electron charge is e, the intensity of the applied external electric field perpendicular to the quantum well plane is F, and the dielectric constant of the structure is ϵ. Using the trial wave function of Eq. (2) and Hamiltonian [Eq. (3)], we solved the static Schrödinger equation iteratively, obtaining the electron and hole wave functions from which the exciton energy E_{ex} and relative oscillator strength f_{rel} are calculated according to the following equations:

$$E_{ex} = \langle \Psi | \mathcal{H} | \Psi \rangle, \quad (4)$$

$$f_{rel} = \frac{\int \Psi_e(z) \Psi_h(z) dz}{\int \Psi_e(z)^{F=0} \Psi_h(z)^{F=0} dz}. \quad (5)$$

Here, the wave functions unperturbed by an external electric field are denoted by the subscript "$F=0$."

Device modeling. Returning to the device proposed in Fig. 1, Fig. 2 shows the results of modeling the triggering of a propagating signal, following a change in the electric potential applied to the first segment. The spatial effects present in the system have been fully accounted for by using the Gross-Pitaevskii equation[18,19] for the polariton field $\psi(\vec{r},t)$,

$$i\hbar \frac{\partial \psi(\vec{r},t)}{\partial t} = \left(\hat{E}_{LP} - \frac{i\hbar}{2\tau} + W(\vec{r},t) \right) \psi(\vec{r},t)$$
$$+ \alpha |\psi(\vec{r},t)|^2 \psi(\vec{r},t) + f(\vec{r},t). \quad (6)$$

Here, we neglect the polarization degree of freedom, assuming that the optical excitation $f(\vec{r},t)$ is circularly polarized. The energy of the pump can be accounted for by the inclusion of an oscillatory factor $e^{-i\omega t}$ in the time dependence. $\hat{E}_{LP}$ is the kinetic-energy operator, which should account for the nonparabolic dispersion of polaritons. The eigenvalues of $\hat{E}_{LP}$ can be written in reciprocal space as

$$E_{LP}(\vec{k}) = \frac{E_C(\vec{k}) + E_X(\vec{k})}{2} - \frac{1}{2}\sqrt{[E_C(\vec{k}) - E_X(\vec{k})]^2 + \Omega^2}, \quad (7)$$

where Ω is the Rabi splitting and E_C and E_X are the bare cavity photon and exciton energies, respectively, for which we take parabolic dispersion relations characterized by effective masses m_C and m_X. Returning to Eq. (6), τ represents the polariton lifetime and α represents the strength of polariton-polariton interactions. $W(\vec{r},t)$ is the potential experienced by polaritons, which is spatially dependent due to the metallic structure built into the microcavity design, and is time dependent because of the changes in potential applied to the metallic segments.

Equation (6) can be solved numerically with the initial condition $\psi(\vec{r},t=0)=0$. In our calculations we used the following parameters, typical for state-of-the-art GaAs-based microcavities:[7] Ω = 10 meV, $m_C = 3 \times 10^{-5} m$ (m is the free-electron mass), $m_X = 0.22m$, $\tau = 3$ ps, $\Delta_0 = 0.5$ meV, $\Delta_1 = 0.4$ meV, and $\Delta_2 = 0.8$ meV. It was assumed that the metal strip causes a 5 meV redshift of the TPEPM beneath it with respect to the lowest-energy exciton-polariton mode elsewhere.

In Fig. 2 it is apparent that the signal propagates across all four segments. The signal propagation observed in Fig. 2 is dependent on maintaining the potential bias in the second, third, and fourth segments so that the detuning remains as Δ_0. If we were to switch the potential in the third segment so that the local detuning had the substantially larger value of Δ_2, corresponding to the (blue) dotted curve in Fig. 1(b), the signal would not be able to propagate between the second and fourth segments. The results of modeling this case are shown in Fig. 3 and demonstrate that the device can behave as an electro-optic transistor in which the optical signal is electrically controlled. The whole device can be reset by temporarily applying a potential corresponding to a detuning of Δ_2 to all segments.

Other functionalities are also straightforward to produce using polariton neurons. Signals can be duplicated by splitting channels or combined in OR logic gates simply by combining channels.[8] Polariton neurons are also able to link multiple elements in a circuit together, a facility not afforded by many other optical logic element concepts. Without requiring external optics (other than a single broad excitation field) a polariton neuron-based optical circuit fits comfortably into a single compact microcavity. Typically each element in the optical circuit functions on a time scale of 100–200 ps cor-
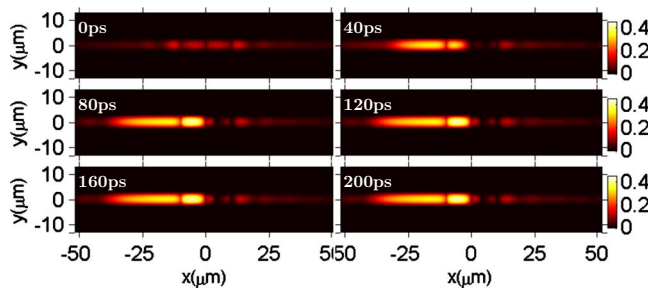
FIG. 3. (Color online) The same situation as in Fig. 2 but a potential is also applied to the third segment, such that the pump-polariton detuning there is $\Delta_2 = 0.8$ meV, and blocks the signal propagation along the polariton neuron.

responding to a repetition rate of 5–10 GHz. The power requirements are also favorable; the high strength of exciton-exciton interactions makes it possible to achieve the nonlinear regime needed for bistability with relatively low optical power. For example, a power of 2.8 mW has been used to achieve bistability in GaAs-based microcavities.[13] Future samples, perhaps based on GaN, are expected to operate at even lower powers, partly due to the increased exciton-exciton interaction strength and partly due to higher cavity Q factors.

We have shown how the electrical sensitivity of optical bistability in semiconductor microcavities could be used to construct a new generation of electro-optical devices with compact size and low power consumption. Although we have focused on fully integrated electro-optical logic circuits, it is

also possible to imagine using the electrical control of polariton intensity as the basis of bistable memory devices, which could switch on time scales on the order of the polariton lifetime (~ 3 ps) and have long memory lifetimes, at least as long as the laser coherence time. In another application, a suitably patterned metallic structure could provide the spatial control to produce an array of bistable elements acting as a spatial light modulator. It is also worth noting that spatial phase coherence can be naturally attained from the spatial coherence of the laser, suggesting that microcavities could also find application in phase array optics.

An important new functionality of polariton integrated circuits may be achieved by taking advantage of the polarization degree of freedom of exciton-polaritons.[20] The polarization multistability (i.e., coexistence of right-circularly, left-circularly, and linearly polarized stable states[12]) makes possible the realization of schemes with encoding above binary logic. A theoretical proposal for all-optical polariton polarization switches[8] has been recently demonstrated experimentally.[14]

In conclusion, until recently, semiconductor microcavities have been considered almost exclusively for applications in solid-state optical sources.[6,21] However, now it is apparent that they are extremely promising as the basis of devices with applications in ultrafast information processing. Indeed, it is clear that we have only just begun to appreciate the potential of cavity plasmon–exciton-polariton systems.

[1] A. V. Kavokin, J. J. Baumberg, G. Malpuech, and F. P. Laussy, *Microcavities* (Oxford University Press, Oxford, 2007).

[2] J. Kasprzak, M. Richard, S. Kundermann, A. Baas, P. Jeambrun, J. M. J. Keeling, F. M. Marchetti, M. H. Szymańska, R. André, J. L. Staehli, V. Savona, P. B. Littlewood, B. Deveaud, and Le Si Dang, Nature (London) **443**, 409 (2006).

[3] R. Balili, V. Hartwell, D. Snoke, L. Pfeiffer, and K. West, Science **316**, 1007 (2007).

[4] C. W. Lai, N. Y. Kim, S. Utsunomiya, G. Roumpos, H. Deng, M. D. Fraser, T. Byrnes, P. Recher, N. Kumada, T. Fujisawa, and Y. Yamamoto, Nature (London) **450**, 529 (2007).

[5] A. Amo, J. Lefrère, S. Pigeon, C. Adrados, C. Ciuti, I. Carusotto, R. Houdré, E. Giacobino, and A. Bramati, Nat. Phys. **5**, 805 (2009).

[6] S. I. Tsintzos, N. T. Pelekanos, G. Konstantinidis, Z. Hatzopoulos, and P. G. Savvidis, Nature (London) **453**, 372 (2008).

[7] D. Bajoni, E. Semenova, A. Lemaître, S. Bouchoule, E. Wertz, P. Senellart, S. Barbay, R. Kuszelewicz, and J. Bloch, Phys. Rev. Lett. **101**, 266402 (2008).

[8] T. C. H. Liew, A. V. Kavokin, and I. A. Shelykh, Phys. Rev. Lett. **101**, 016402 (2008).

[9] C. Symonds, A. Lemaître, E. Homeyer, J. C. Plenet, and J. Bellessa, Appl. Phys. Lett. **95**, 151114 (2009).

[10] M. E. Sasin, R. P. Seisyan, M. A. Kalitteevski, S. Brand, R. A. Abram, J. M. Chamberlain, A. Yu. Egorov, A. P. Vasil'ev, V. S. Mikhrin, and A. V. Kavokin, Appl. Phys. Lett. **92**, 251112

(2008).

[11] M. Kaliteevski, S. Brand, R. A. Abram, I. Iorsh, A. V. Kavokin, and I. A. Shelykh, Appl. Phys. Lett. **95**, 251108 (2009).

[12] N. A. Gippius, I. A. Shelykh, D. D. Solnyshkov, S. S. Gavrilov, Yuri G. Rubo, A. V. Kavokin, S. G. Tikhodeev, and G. Malpuech, Phys. Rev. Lett. **98**, 236401 (2007).

[13] A. Baas, J. Ph. Karr, H. Eleuch, and E. Giacobino, Phys. Rev. A **69**, 023809 (2004).

[14] A. Amo, T. C. H. Liew, C. Adrados, R. Houdré, E. Giacobino, A. V. Kavokin, and A. Bramati, Nature Photon. **4**, 361 (2010).

[15] G. Bastard, E. E. Mendez, L. L. Chang, and L. Esaki, Phys. Rev. B **28**, 3241 (1983).

[16] D. A. B. Miller, D. S. Chemla, T. C. Damen, A. C. Gossard, W. Wiegmann, T. H. Wood, and C. A. Burrus, Phys. Rev. B **32**, 1043 (1985).

[17] H.-J. Polland, L. Schultheis, J. Kuhl, E. O. Göbel, and C. W. Tu, Phys. Rev. Lett. **55**, 2610 (1985).

[18] I. Carusotto and C. Ciuti, Phys. Rev. Lett. **93**, 166401 (2004).

[19] M. Wouters, I. Carusotto, and C. Ciuti, Phys. Rev. B **77**, 115340 (2008).

[20] I. A. Shelykh, A. V. Kavokin, Yu. G. Rubo, T. C. H. Liew, and G. Malpuech, Semicond. Sci. Technol. **25**, 013001 (2010).

[21] S. Christopoulos, G. Baldassarri Höger von Högersthal, A. J. D. Grundy, P. G. Lagoudakis, A. V. Kavokin, J. J. Baumberg, G. Christmann, R. Butté, E. Feltin, J.-F. Carlin, and N. Grandjean, Phys. Rev. Lett. **98**, 126405 (2007).